FE-BI-MLFMA Combined with FETI for Accurate and Fast Computation of Scattering by Large-Scale Finite Array Structure

Hong-Wei Gao, Li Gong, Ming-Lin Yang, and Xin-Qing Sheng
Center for Electromagnetic Simulation,
School of Information and Electronics, Beijing Institute of Technology, Beijing, 100081 China.

Abstract-**To effectively solve the electromagnetic scattering problem of large-scale finite array structure, a non-overlapping domain decomposition method(DDM), the dual-primal finite element tearing and interconnecting method(FETI-DP), is applied to the hybrid finite element–boundary integral–multilevel fast multipole algorithm method(FE-BI-MLFMA). The formula of near scattering field is deduced by equivalent electric and magnetic current. Then, the Generalized Radar Cross Section (GRCS) in near scattering region is calculated by the near scattering field. The numerical performance of the proposed method is demonstrated by calculating a patch antenna array's scattering.**

I. INTRODUCTION

The domain Decomposition Method (DDM) has always been recognized as an important scheme to construct highly efficient algorithm. The Finite Element Method (FEM), implemented together with a domain decomposition algorithm in electromagnetic, was first introduced by Despr és[1]. Subsequently, sorts of advanced finite element domain decomposition methods were proposed [2]-[6]. Among various existing finite element domain decomposition methods, a non-overlapping finite element tearing and interconnection (FETI) method is investigated as a particularly efficient method [2]-[3]. Recently, a dual-primal technology is adopted in FETI denoted as FETI-DPEM1, which is successful applied for the computation of large-scale finite array antenna radiation problem [5]. The convergence of the FETI-DPEM1 algorithm becomes slow at higher frequencies. This disadvantage can be eliminated by using the FETI-DPEM2 algorithm [6], which enhances the dual-primal (DP) idea with two Lagrange multipliers, while the field continuity at the subdomain interfaces is guaranteed by the Robin-type transmission condition. To improve the algorithm [6] accuracy, a second-order absorbing condition is introduced [7], but the approximation for the solution can't be omitted completely.

The hybrid finite element–boundary integral–multilevel fast multipole algorithm method (FE-BI-MLFMA) has been verified as a general and accurate method for inhomogeneous electromagnetic problems [8]. Whereas, the final deduced FE-BI matrix is an ill-conditioned matrix for its partly sparse and partly dense matrix. It becomes difficult to solve the system matrix by general iterative solver and even no convergence for some complex problems. Then, two methods are applied to improve the convergence of traditional FE-BI-MLFMA [9]-[10]. Though the two methods can accelerate the convergence effectively, the process of solving the inverse of a sparse matrix required in each method consumes large memory. This bottleneck limits the application of FE-BI-MLFMA in solving large-scale electromagnetic problems.

To improve the computational accuracy of finite element DDM and reduce the high memory consumption by FE-BI-MLFMA, combining the dual-primal tearing and interconnecting DDM and FE-BI-MLFMA together yields a new hybrid method denoted as FETI-BI-MLFMA. What's more, scattering field anywhere in space is strictly deduced by the current and magnetic sources on the outward surface of object which has been obtained by FETI-BI-MLFMA. Take a patch array antenna as an example of finite array structure and calculate its near and far field by the proposed method.

II. FORMULATION

A. The FETI-BI-MLFMA Method

Considering scattering by an inhomogeneous object, whose surface is denoted as S .According to the conventional FE-BI-MLFMA [8], the computing region is directly divided into interior region and exterior boundary by the surface S .The interior field is formulated as

$$F(\mathbf{E}) = \frac{1}{2}\int_V \left[(\nabla \times \mathbf{E})\cdot\left([\mu_r]^{-1}\nabla \times \mathbf{E}\right) - k_0^2\mathbf{E}\cdot[\varepsilon_r]\mathbf{E} \right]dV + jk_0\int_s (\mathbf{E}\times\bar{\mathbf{H}})\cdot\hat{n}dS \quad (1)$$

Here, $\bar{\mathbf{H}} = Z_0\mathbf{H}$ where $\mathbf{E}$ and $\mathbf{H}$ are the unknown electric and magnetic field respectively. In addition, Z_0 is the free-space impedance and k_0 is the free-space wave number. $\hat{n}$ denotes the outward unit vector normal to S . The field on the exterior surface is formulated into the following combined field integral equation (CFIE):

$$0.5\times\text{EFIE}+0.5\times\text{MFIE} \quad (2)$$

For explicit expressions of the function CFIE in (2), the reader should refer to [8].

In this paper, the FETI-DPEM2 algorithm is applied in the FEM part of FE-BI-MLFMA. To be more specific, the interior FEM domain is decomposed into N non-overlapping sub-domains. Let the sub-domains V_i and V_j be adjacent, we employ $\Gamma_{j,i}$, $\Gamma_{i,j}$ to represent their respective neighboring surfaces, with the corresponding outward unit normal vectors being $\hat{n}_i$ and $\hat{n}_j$ .The edges shared by more than two subdomains

or shared by two sub-domains only for those on exterior boundary are called corner edges denoted as Γ_c.

At the interfaces Γ_i, the continuity of the tangential electric and magnetic field components is guaranteed by imposing Robin-type transmission conditions with extra variable Λ_i:

$$\hat{n}_i \times \left(\left[\mu_{r,i} \right]^{-1} \cdot (\nabla \times \mathbf{E}_i) \right) + jk_0 (\hat{n}_i \times \hat{n}_i \times \mathbf{E}_i) = \Lambda_i \quad on \ \Gamma_i \tag{3}$$

Thus the fields in each sub-domain can be independently formulated with combination of (1) and (3), which is given by

$$F(\mathbf{E}_i) = \frac{1}{2} \int_{V_i} \left[(\nabla \times \mathbf{E}_i) \cdot \left(\left[\mu_{r,i} \right]^{-1} \nabla \times \mathbf{E}_i \right) - k_0^2 \mathbf{E}_i \cdot \left[\varepsilon_{r,i} \right] \mathbf{E}_i \right] dV + \\ \alpha \int_{\Gamma_i} (\hat{n}_i \times \mathbf{E}_i) \cdot (\hat{n}_i \times \mathbf{E}_i) dS + \int_{\Gamma_i} \mathbf{E}_i \cdot \Lambda_i dS + jk_0 \int_{s_i} (\mathbf{E}_i \times \bar{\mathbf{H}}_i) \cdot \hat{n}_i dS \tag{4}$$

The electric field $\mathbf{E}_i$ in the ith sub-domain can be expanded with edge-element vector basis function and (4) is cast in the following form for the ith sub-domain:

$$\mathbf{K}_i E_i = -\mathbf{C} \bar{H}_{s,i} - \int_{\Gamma_i} \mathbf{W}_i \cdot \Lambda_i dS \tag{5}$$

where

$$\mathbf{K}_i = \int_{V_i} \left[(\nabla \times \mathbf{W}_i) \cdot \left[\mu_{r,i} \right]^{-1} (\nabla \times \mathbf{W}_i)^{\mathrm{T}} - k_0^2 \mathbf{W}_i \cdot \left[\varepsilon_{r,i} \right] \mathbf{W}_i^{\mathrm{T}} \right] dV \\ + \alpha \int_{\Gamma_i} (\hat{n}_i \times \mathbf{W}_i) \cdot (\hat{n}_i \times \mathbf{W}_i)^{\mathrm{T}} dS \tag{6}$$

$$\mathbf{C} = jk_0 \int_{s_i} (\mathbf{W}_i \times \mathbf{W}_i^{\mathrm{T}}) \cdot \hat{n}_i dS \tag{7}$$

with $\mathbf{W}_i$ denotes a column vector containing the edge-element vector basis function in the ith sub-domain.

In each subdomain, the unknown coefficients of the electric field E_i are grouped into three categories $E_{V,i}$, $E_{I,i}$, and $E_{c,i}$:

$$E_i = \left[E_{V,i}^{\mathrm{T}}, E_{I,i}^{\mathrm{T}}, E_{c,i}^{\mathrm{T}} \right]^{\mathrm{T}} = \left[E_{r,i}^{\mathrm{T}}, E_{c,i}^{\mathrm{T}} \right]^{\mathrm{T}} \tag{8}$$

In (8), the superscript T denotes matrix transposition. Furthermore, the subscripts *V, I* and *c* denote the degrees of freedom associated with the internal volume, interface, and corner edges, respectively. The unknowns $E_{r,i}$ associated with the internal volume and interfaces are considered as local variables, whereas the unknowns $E_{c,i}$ associated with the corner edges are considered as global variables. The global primal variables in interior FEM region can be represented as:

$$E = \left[E_{r,1}^{\mathrm{T}}, \cdots, E_{r,N}^{\mathrm{T}}, E_c^{\mathrm{T}} \right]^{\mathrm{T}} \tag{9}$$

When the solution vector is constructed in this manner, the tangential electric field at the corner edges is ensured to be continuous. Applying this notation to (5) results in

$$\begin{bmatrix} \mathbf{K}_{rr,i} & \mathbf{K}_{rc,i} \\ \mathbf{K}_{rc,i}^{\mathrm{T}} & \mathbf{K}_{cc,i} \end{bmatrix} \begin{bmatrix} E_{r,i} \\ E_{c,i} \end{bmatrix} = \begin{bmatrix} -\mathbf{B}_{r,i} \mathbf{C}_i \bar{H}_{s,i} - \mathbf{B}_{I,i}^{\mathrm{T}} \lambda_i \\ -\mathbf{B}_{c,i} \mathbf{C}_i \bar{H}_{s,i} \end{bmatrix} \tag{10}$$

Here, $\mathbf{B}_{r,i}$, $\mathbf{B}_{I,i}$, and $\mathbf{B}_{c,i}$ are Boolean matrixes and satisfy $\mathbf{B}_{r,i} E_i = E_{r,i}$, $\mathbf{B}_{I,i} E_{r,i} = E_{I,i}$, and $\mathbf{B}_{c,i} E_i = E_{c,i}$. The unknown λ_i is called the dual-variable and defined as $\left[\mathbf{B}_{I,i}^{\mathrm{T}} \lambda_i \quad 0 \right]^{\mathrm{T}} = \int_{\Gamma_i} \mathbf{W}_i \cdot \Lambda_i dS$ whose dimension corresponds to the number of unknowns at interfaces.

From (10), it can be seen that the system matrix characterizing each subdomain decouples, and the interaction of the adjacent subdomains is included in the transmission conditions of the interfaces. Combining the two matrix equations in (10) permits the elimination of the unknowns $E_{r,i}$. We assemble the subdomains contribution from (10) to obtain a global corner unknowns related system equation written as:

$$\tilde{\mathbf{K}}_{cc} E_c - \tilde{\mathbf{K}}_{cI} \lambda = \tilde{\mathbf{C}}_c \bar{H}_s \tag{11}$$

with

$$\tilde{\mathbf{K}}_{cc} = \sum_{i=1}^{N} \mathbf{O}_{c,i}^{\mathrm{T}} \left(\mathbf{K}_{cc,i} - \mathbf{K}_{rc,i}^{\mathrm{T}} \mathbf{K}_{rr,i}^{-1} \mathbf{K}_{rc,i} \right) \mathbf{O}_{c,i} \tag{12}$$

$$\tilde{\mathbf{C}}_c = \sum_{i=1}^{N} \mathbf{O}_{c,i}^{\mathrm{T}} \left(\mathbf{K}_{rc,i}^{\mathrm{T}} \mathbf{K}_{rr,i}^{-1} \mathbf{B}_{r,i} \mathbf{C}_i - \mathbf{B}_{c,i} \mathbf{C}_i \right) \mathbf{R}_i \tag{13}$$

$$\tilde{\mathbf{K}}_{cI} = \sum_{i=1}^{N} \mathbf{O}_{c,i}^{\mathrm{T}} \mathbf{K}_{rc,i}^{\mathrm{T}} \mathbf{K}_{rr,i}^{-1} \mathbf{B}_{I,i}^{\mathrm{T}} \mathbf{O}_{I,i} \tag{14}$$

where $\mathbf{O}_{c,i}$, $\mathbf{O}_{I,i}$, and $\mathbf{R}_i$ are Boolean matrices satisfying $E_{c,i} = \mathbf{O}_{c,i} E_c$, $\lambda_i = \mathbf{O}_{I,i} \lambda$, $\bar{H}_{s,i} = \mathbf{R}_i \bar{H}_s$.

To couple subdomains together, another set of equations representing the tangential electric and magnetic field continuity across the interfaces between different subdomains is required. Based on Robin-type transmission condition given by (3) at interface $\Gamma_{j,i}$, we can get

$$\lambda_{j,i} + \lambda_{i,j} = -2\mathbf{M}_{i,j} E_{i,j} \quad i = 1,2,\cdots N \text{ and } j \in \text{neighbour}(i) \tag{15}$$

Where $E_{i,j}$ denotes the electric field at the interface of the jth subdomain adjacent to the ith subdomain and $\mathbf{M}_{i,j} = jk_0 \int_{\Gamma_{i,j}} (\hat{n}_i \times \mathbf{W}_i) \cdot (\hat{n}_j \times \mathbf{W}_j)^{\mathrm{T}} dS$.

Assembling (15) together for all sub-domains to get the following another corner problem equation:

$$\tilde{\mathbf{K}}_{II} \lambda + \tilde{\mathbf{K}}_{Ic} E_c = \tilde{\mathbf{C}}_I \bar{H}_s \tag{16}$$

with

$$\tilde{\mathbf{K}}_{II} = \mathbf{I} + \sum_{i=1}^{N} \mathbf{O}_{I,i}^{\mathrm{T}} \sum_{j \in \text{neighbor}(i)} \mathbf{T}_{j,i}^{\mathrm{T}} (\mathbf{T}_{i,j} - 2\mathbf{M}_{j,i} \mathbf{T}_{i,j} \mathbf{B}_{I,j} \mathbf{K}_{rr,j}^{-1} \mathbf{B}_{I,j}^{\mathrm{T}}) \mathbf{O}_{I,j} \tag{17}$$

$$\tilde{\mathbf{K}}_{Ic} = \sum_{i=1}^{N} \mathbf{O}_{I,i}^{\mathrm{T}} \sum_{j \in \text{neighbor}(i)} \mathbf{T}_{j,i}^{\mathrm{T}} (-2\mathbf{M}_{i,j} \mathbf{T}_{i,j} \mathbf{B}_{I,j} \mathbf{K}_{rr,j}^{-1} \mathbf{K}_{rc,j}) \mathbf{O}_{c,j} \tag{18}$$

$$\tilde{\mathbf{C}}_I = \sum_{i=1}^{N} \mathbf{O}_{I,i}^{\mathrm{T}} \sum_{j \in \text{neighbor}(i)} \mathbf{T}_{j,i}^{\mathrm{T}} (2\mathbf{M}_{i,j} \mathbf{T}_{i,j} \mathbf{B}_{I,j} \mathbf{K}_{rr,j}^{-1} \mathbf{B}_{r,j} \mathbf{C}_j) \mathbf{R}_j \tag{19}$$

And Boolean matrix $\mathbf{T}_{j,i}$ satisfies $E_{j,i} = \mathbf{T}_{j,i} E_i$ and $\lambda_{j,i} = \mathbf{T}_{j,i} \lambda_i$.

By combining (11) and (16) and eliminating E_c, we can derive the equation for the dual unknowns and the magnetic field on surface s

$$\left(\tilde{\mathbf{K}}_{II} + \tilde{\mathbf{K}}_{Ic} \tilde{\mathbf{K}}_{cc}^{-1} \tilde{\mathbf{K}}_{cI} \right) \lambda + \left(\tilde{\mathbf{K}}_{Ic} \tilde{\mathbf{K}}_{cc}^{-1} \tilde{\mathbf{C}}_c - \tilde{\mathbf{C}}_I \right) \bar{H}_s = 0 \tag{20}$$

For the sake of clarity, let

$$\tilde{\mathbf{D}} = \tilde{\mathbf{K}}_{II} + \tilde{\mathbf{K}}_{Ic} \tilde{\mathbf{K}}_{cc}^{-1} \tilde{\mathbf{K}}_{cI} \tag{21}$$

$$\tilde{\mathbf{F}} = \tilde{\mathbf{K}}_{Ic} \tilde{\mathbf{K}}_{cc}^{-1} \tilde{\mathbf{C}}_c - \tilde{\mathbf{C}}_I \tag{22}$$

Therefore, (20) takes the form

$$\tilde{\mathbf{D}} \lambda + \tilde{\mathbf{F}} \bar{H}_s = 0 \tag{23}$$

Similar to the convenient FE-BI-MLFMA, discretizing (2) by MOM yields:

$$\mathbf{P} E_s + \mathbf{Q} \bar{H}_s = \mathbf{b} \tag{24}$$

For explicit expressions of the matrix $\mathbf{P}$, $\mathbf{Q}$ and column vector $\mathbf{b}$ in (24), the reader should refer to [8].

Because of (9), the unknown E_s is grouped into $E_{c,s}$ and $E_{r,s}$ .with the aid of (10) and (11), equation (24) is deduced into

$$\tilde{\mathbf{P}} \lambda + \tilde{\mathbf{Q}} \bar{H}_s = \mathbf{b} \tag{25}$$

where

$$\tilde{\mathbf{P}} = \mathbf{P} \left[\mathbf{O}_{c,s}^{\mathrm{T}} \tilde{\mathbf{K}}_{cc}^{-1} \tilde{\mathbf{K}}_{cI} - \sum_{i=1}^{N} \mathbf{B}_{sr,i} (\mathbf{K}_{rr,i}^{-1} \mathbf{K}_{rc,i} \mathbf{O}_{c,i} \tilde{\mathbf{K}}_{cc}^{-1} \tilde{\mathbf{K}}_{cI} + \mathbf{K}_{rr,i}^{-1} \mathbf{B}_{I,i}^{\mathrm{T}} \mathbf{O}_{I,i}) \right] \tag{26}$$

$$\tilde{\mathbf{Q}} = \mathbf{Q} + \mathbf{P}\left[\mathbf{O}_{c,s}^{\mathrm{T}} \tilde{\mathbf{K}}_{cc}^{-1} \tilde{\mathbf{C}}_c - \sum_{i=1}^{N} \mathbf{B}_{sr,i} (\mathbf{K}_{rr,i}^{-1} \mathbf{K}_{rc,i} \mathbf{O}_{c,i} \tilde{\mathbf{K}}_{cc}^{-1} \tilde{\mathbf{C}}_c + \mathbf{K}_{rr,i}^{-1} \mathbf{B}_{r,i} \mathbf{C}_i \mathbf{R}_i) \right] \quad (27)$$

The final system matrix equation of FETI-BI-MLFMA is obtained by combination of (23) and (25) as

$$\begin{bmatrix} \tilde{\mathbf{D}} & \tilde{\mathbf{F}} \\ \tilde{\mathbf{P}} & \tilde{\mathbf{Q}} \end{bmatrix} \begin{bmatrix} \lambda \\ \bar{H}_s \end{bmatrix} = \begin{bmatrix} 0 \\ \mathbf{b} \end{bmatrix} \quad (28)$$

Observing (28), by the introduction of the dual unknown λ, the original 3-D problem is reduced to a problem relating with sub-domain interfaces and exterior boundary surface. It is apparent that the problem always has fewer unknowns which enable us to solve large-scale problems.

B. The Strict Scattering Field Formulation

After solved by FETI-BI-MLFMA, the fields in interior region and on surface S have been obtained. Because the obtained filed is limited in computing region, scattering field anywhere in space out of objects can be strictly deduced by the current and magnetic sources on surface S according to electromagnetic field theory. The scattering electric field $\mathbf{E}^s$ in $\mathbf{r}$ is calculated by

$$\mathbf{E}^s(\mathbf{r}) = Z\mathrm{L}(\hat{n} \times \mathbf{H}_s) - \mathrm{K}(\mathbf{E}_S \times \hat{n}) \quad (29)$$

where $Z = \sqrt{\mu/\varepsilon}$. L and K are two operators defined in [11]. Introduce $\mathbf{R} = \mathbf{r} - \mathbf{r}'$, $R = |\mathbf{r} - \mathbf{r}'|$, and $\hat{R} = \mathbf{R}/R$ where $\mathbf{r}'$ denotes any point at surface S. Through a series of mathematical transformation, formula (29) is reduced to

$$\mathbf{E}^s(\mathbf{r}) = \frac{jkZ_0}{4\pi} \int_S \frac{(\hat{n} \times \mathbf{H}_s(\mathbf{r}') \times \mathbf{R}) \times \mathbf{R}e^{-jkR}}{R^3} \left(1 + \frac{1}{jkR} - \frac{1}{k^2R^2}\right) dS$$
$$+ \frac{Z_0}{2\pi} \int_S \frac{(\hat{n} \times \mathbf{H}_s(\mathbf{r}') \cdot \mathbf{R}) \mathbf{R}e^{-jkR}}{R^4} \left(1 + \frac{1}{jkR}\right) dS \quad (30)$$
$$- \frac{jk}{4\pi} \int_S \frac{\mathbf{E}_s(\mathbf{r}') \times \hat{n} \times \mathbf{R}e^{-jkR}}{R^2} (1 + \frac{1}{jkR}) dS$$

Using (30), the scattering electric filed in near and far region is strictly calculated, we adopt the following general radar cross section (GRCS) [12] to further demonstrate object's near and far field property.

$$GRCS = 4\pi R^2 \frac{\left|\mathbf{E}^s \cdot \hat{e}_r\right|^2}{\left|\mathbf{E}^i\right|^2} \quad (31)$$

In formula (31), $\hat{e}_r$ denotes the polarized direction, R denotes the distance between observing point and center of target. When R is big enough, GRCS is consistent with the strict RCS.

III. NUMERICAL EXPERIMENTS

To verify the validity of FETI-BI-MLFMA and strict scattering formulation, a homogeneous dielectric $4\lambda \times 4\lambda \times 4\lambda$ cube's GRCS on sphere surface 1000λ away from the center of object is calculated. It is illuminated by plane wave at incidence angle $\theta = 0°, \varphi = 0°$ and the computing region is divided by cuboid subdomain with dimension of $0.5\lambda \times 0.5\lambda \times 4\lambda$. A tetrahedral mesh with average edge length of 0.05λ is used. The result from FETI-BI-MLFMA is compared with RCS by MOM in Fig. 1. Investigate Fig. 1 the result from FETI-BI-MLFMA has a good agreement with MOM.
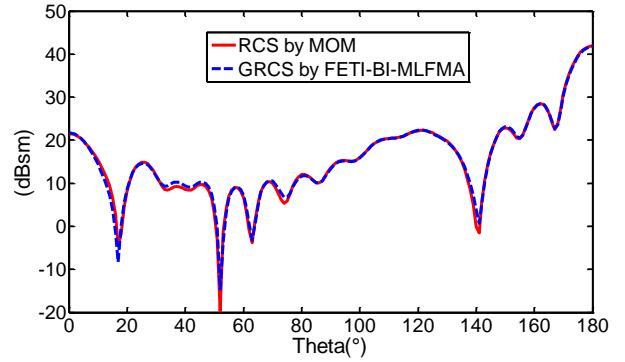

Fig. 1. Bi-static VV-polarized RCS and GRCS of a dielectric cube in the E-plane
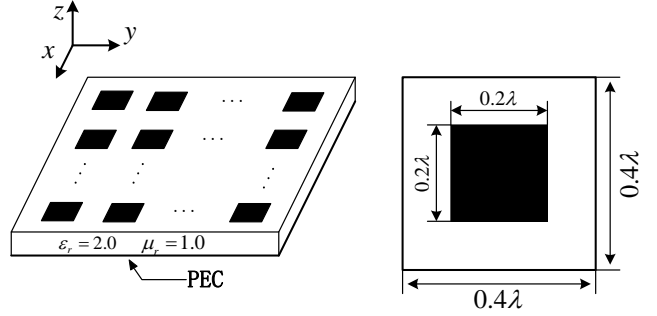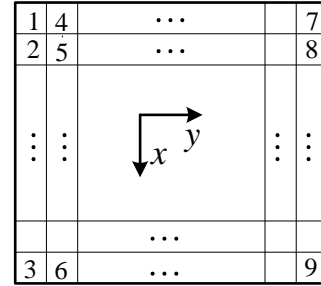

Fig. 2. Illustration of a patch antenna array

Fig. 3. Illustration of different subdomains needed to be analyzed in $M \times N$ array problem

Next, take a patch array antenna's (Fig. 2) scattering as an example of finite array structure to investigate the numerical scalability of FETI-BI-MLFMA. Each patch element is regarded as a sub-domain and is extended along both x and y directions denoted as $M \times N$ patch array antenna. A tetrahedral mesh with average edge length of 0.05λ is used. To save computer memory and time, the periodicity of structure is sufficiently utilized which is shown by Fig. 3. 8×8, 16×16, 32×32 patch array antennas are illuminated by plane wave at incidence angle $\theta = 0°, \varphi = 0°$ and the GRCS on sphere surface 1000λ away from the center of objects is calculated. Results are showed in Fig.4-6 and mainly computation information is listed in Table I Table I suggests that memory consumption is rising linearly with the increase of sub-domain number, and the iterative step goes up at a very slow speed, which demonstrating the favorable numerical scalability of FETI-BI-MLFMA for solving two-dimension extension problems.
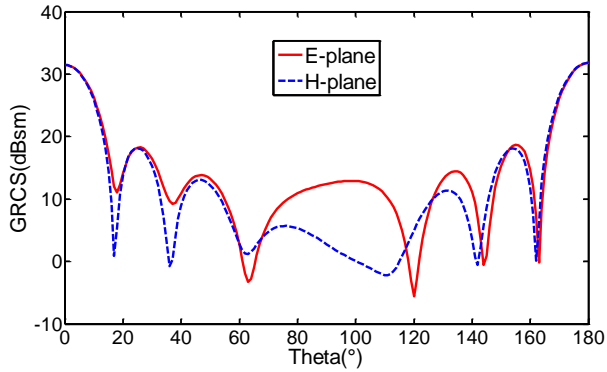
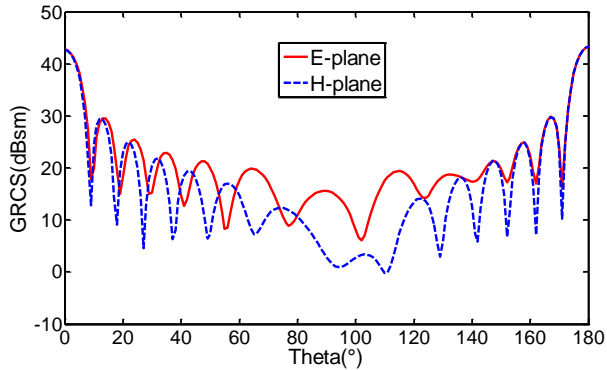Fig. 4. Bi-static GRCS of the 8×8 patch antenna array

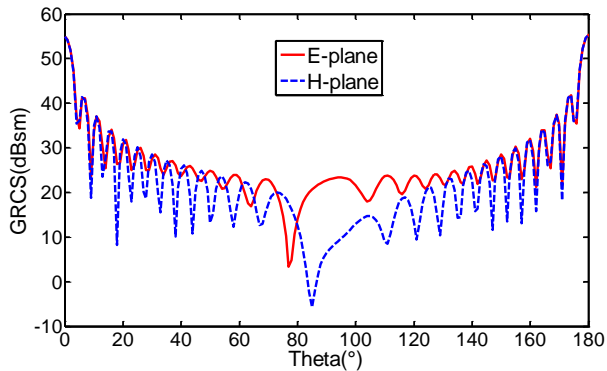Fig. 5. Bi-static GRCS of the 16×16 patch antenna array

Fig. 6. Bi-static GRCS of the 32×32 patch antenna array

TABLE I
COMPUTATION INFORMATION FOR PATCH ANTENNA ARRAYS

Array size	Iteration number	Memory （GB）	Computing time （min）
8×8	50	0.5	5.2
16×16	87	1.9	23.8
32×32	145	7.6	153.9

Finally, we use the presented method to calculate GRCS by 50×50 patch antenna array on sphere surface 15λ, 20λ, and 30λ away from the center of object. The driving plane wave is at incidence angle $\theta = 0^\circ, \varphi = 0^\circ$. Fig. 7 shows the computational result.
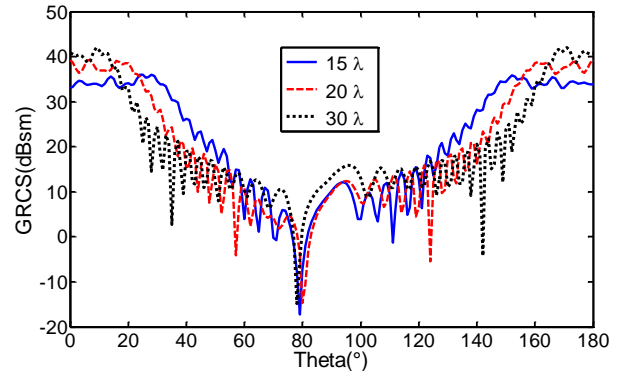

Fig. 7 Bi-static VV-polarized GRCS of the 50×50 patch array antenna in E-plane

REFERENCES

[1] B. Despres, P. Joly, and J. E. Roberts, "A domain decomposition method for the harmonic Maxwell equation," in *iterative Methods in linear Algebra. Amsterdam*, The Netherlands: Elsevier, 1992, pp. 475-484
[2] C. Farhat and F. Roux, "A method of finite element tearing and inter connecting and its parallel solution algorithm,"Int. J. Number.Method. Eng., vol. 32, pp. 1205-1227, Oct. 1991.
[3] C. T. Wolfe, U. Navsariwala, and S. D. Gedney, "A parallel finite-element tearing and interconnecting algorithm for solution of the vectorwave equation with PML absorbing medium," *IEEE Trans. AntennasPropagat.*, vol. 48, pp. 278–284, Feb. 2000.
[4] M. N. Vouvakis, Z. Cendes, and J.F.Lee, "A FEM domain decomposition method for photonic and electromagnetic band gap structures," *IEEE Trans. Antennas Propagat.*, vol. 54, no. 2, pp. 721–733, Feb. 2006.
[5] Y. J. Li and J. M. Jin, "A vector dual-primal finite element tearing and interconnecting method for solving 3D large-scale electromagnetic problems," *IEEE Trans. Antennas Propagat.*, vol. 54, pp. 3000-3009, Oct. 2006.
[6] Y. J. Li, J. M. Jin, "A new dual-primal domain decomposition approach for finite element simulation of 3-D large-scale electromagnetic problems," I*EEE Trans. Antennas Propagat.*, vol. 55, pp. 2803-2810, Oct. 2007.
[7] Y. J. Li, J. M. Jin, "Implementation of the Second-Order ABC in the FETI-DPEM Method for 3D EM Problems," *IEEE Trans. Antennas Propagat.*, vol. 56, pp. 5765-5769, Aug. 2008.
[8] X. Q. Sheng, J. M. Song, C. C. Lu, and W. C. Chew, "On the formulation of hybrid finite-element and boundary-integral method for 3D scattering"*, IEEE Trans. Antennas Propagat.*, vol. 46, pp.303-311, Mar. 1998.
[9] J. Liu and J. M. Jin, "A highly effective preconditioner for solving the finite element-boundary integral matrix equation for 3-D scattering, *IEEE Trans. Antennas Propagat.*, vol. 50, pp.1212-1221, Sep. 2002.
[10] X. Q. Sheng and E. K. N. Yung, "Implementation and experiments of a hybrid algorithm of the MLFMA-Enhanced FE-BI method for open-region inhomogeneous electromagnetic problems," *IEEE Trans. Antennas Propagat.*, vol. 50, pp.163-167, Feb. 2002.
[11] X. Q. Sheng, W. Song, *Essentials of computational electromagnetic,*1st ed. Singapore: John Wiley & Sons Singapore Pte. Ltd, 2012
[12] J. M. Taylor,"On the Concept of Near Field Radar Cross Section," *IEEE AP-S Int.Symp.* Dig., 1997, pp. 1172-1175.